Available online at www.sciencedirect.com

ScienceDirect

Energy Procedia 53 (2014) 202 – 213

Energy Procedia

EERA DeepWind'2014, 11th Deep Sea Offshore Wind R&D Conference

Wave influenced wind and the effect on offshore wind turbine performance

Siri Kalvig[a,c]*, Eirik Manger[b], Bjørn H. Hjertager[a], Jasna B. Jakobsen[a]

[a] *University of Stavanger,4036 Stavanger, Norway*
[b] *Acona Flow technology AS, Uniongt. 18, 3732 Skien, Norway*
[c] *StormGeo AS, Nordre Nøstekaien 1, 5011 Bergen, Norway*

Abstract

In this paper the effect of wave influenced wind on offshore wind turbines is studied numerically.The wave is seen as a dynamical roughness that influences the wind flow and hence the wind turbine performance. An actuator line representation of the NREL's 5 MW offshore baseline wind turbine is placed in a simulation domain with a moving mesh that resolves the ocean waves. These wave influenced wind turbine simulations, WIWiTS, show that the wave will influence the wind field at the turbine rotor height. Both the produced power and the tangential forces on the rotor blades will vary according to the three different cases studied: wind aligned with a swell, wind opposing the swell and wind over a surface with low roughness (no waves).

Selection and peer-review under responsibility of SINTEF Energi AS

Keywords: Wave wind interactions, Offshore wind energy, Actuator line, CFD

* Corresponding author. Tel.: +47 91604181
E-mail address: siri.kalvig@uis.no / siri.kalvig@stormgeo.com

Selection and peer-review under responsibility of SINTEF Energi AS
doi:10.1016/j.egypro.2014.07.229

1. Introduction

Ocean surface waves develop due to the frictional drag over the water's surface. Momentum from the air is transported to the ocean during the wave development, but the waves themselves will also influence the wind field. This process is often ignored, both in weather forecasting and in the field of offshore wind energy [1]. Different sea states affect the wind field in various ways. Wave shape, wave age and wave direction are important for upward momentum transfer in the marine atmospheric boundary layer (MABL) [2]. It is common to divide the wave regime into two parts: wind-waves are locally generated by the wind and swells are waves that have propagated away from the source origin. While wind-waves are often aligned with the wind, the swell direction is not necessarily correlated with the wind direction. Occasionally, swells will oppose the wind field, and this is known to give rise to interesting situations with increased turbulence levels over the sea surface [3]. Although it is known that fast moving waves in a low wind regime will influence the whole depth of the MABL, it is still uncertain to what extent the wave induced wind field will affect an offshore wind turbine or a wind farm [1].

In this paper, we present a numerical study of the possible effects wave states may have on the wind field and the following indirect effect on an offshore wind turbine. This is done by using computational fluid dynamics (CFD). In these CFD simulations the air flow does not influence the waves themselves. The wave is prescribed as a solid moving ground. Therefore this is a study of the wave *influenced* wind and the possible effect on offshore wind turbine performance.

2. Wave influenced wind

The wind profile over a surface is influenced by the roughness of the surface and the atmospheric stability. Wind observations at different heights are limited in offshore environments. Therefore wind speed profile models are frequently used to extrapolate the wind speed observations at lower levels to the wind turbine hub height or the swept rotor area. Small deviations from the real wind speed will significantly influence the anticipated wind power levels which are proportional to the cube of the wind speed. Different wind profiles will also give rise to different loads on the blade and the rotor nacelle assembly [4]. Therefore a correct description of the wind profile is of outmost importance for both for wind turbine design, wind assessment and wind energy harvest.

Expression for the wind profile can be found by using Monin-Obukhov similarity theory (MOST). MOST is valid in the constant flux layer (where the fluxes are assumed to vary little with height). Under neutral atmospheric stability conditions MOST theory leads to the logarithmic wind profile [5]:

$$U(z) = \left(\frac{u_*}{k}\right) ln\left(\frac{z}{z_0}\right) \quad (1)$$

where k = 0.4 is the von Kármán's constant, z_0 is the roughness length (defined as the height where the wind speed equals zero) and u_* is the friction velocity. The friction velocity is defined as [5],

$$u_*^{\,2} = \frac{\tau_0}{\rho}, \quad (2)$$

where τ_0 is the force per unit area exerted by the ground surface on the flow and ρ is the density of the air. The roughness length, z_0, can be derived from wind speed measurements. The literature contains different recommendations for selection of z_0 for different surfaces. In the field of offshore wind industry the sea surface is generally considered as levelled and smooth, and, therefore, a low z_0 value of 0.0002 m is often chosen [6]. This is also the value of the roughness used in the simulations described later in this paper.

Atmospheric stability is of importance when studying the wind profiles and it has also been documented that both energy yield and fatigue damage on a wind turbine differ when atmospheric stability is taken into consideration [7,8]. Nevertheless, in this study, we have assumed neutral atmospheric stratification; hence there will be no heat exchange between the sea surface and the overlying air.

The waves can be seen as a dynamical roughness of the sea surface. Different sea states and different directions of the waves, relative to the wind direction, will give rise to different perceived sea surface roughness. The ratio between the phase speed (c_p) of the waves at the peak of the wave spectrum and the wind speed at 10 m, adjusted to neutral conditions (U_{10N}), is called the wave age (χ_{10}) [9];

$$\chi_{10} = \frac{c_p}{U_{10N}}, \tag{3}$$

This can be a useful parameter when classifying different wave regimes because wave ages for young seas (associated with locally generated wind waves and developing seas) are smaller than those for old seas (associated with faster moving swell and decaying seas). When χ_{10} is 1.2 the wave field is believed to be fully developed. Young wind seas have a wave age that is characterised by $\chi_{10} < 1.2$ and a swell dominated wave field by $\chi_{10} > 1.2$ [9]. In this paper, two different swells with wave age of 1.5 and 2.1 are investigated and coupled with wind turbine performance modelling.

3. Wind turbine performance modelling

Wave loads, corrosion and marine organic growth affect the offshore wind turbines and this is covered in the governing standards for offshore wind turbines. There are however, no considerations of how the sea state itself can affect the wind profile and the turbulence in the MABL and the following possible indirect effect of waves on the rotor-nacelle assembly [1].

The basis for the wind turbine performance in this paper is the actuator line methodology of Sørensen and Shen [10]. Here the rotor blades are represented as span-wise sections with airfoil characteristics, and the blade loading is implemented in the spanwise sections and introduced in the Navier-Stokes equations as a body force. Data and description of the National Renewable Energy Laboratory's (NREL) offshore baseline wind turbine, the NREL 5 MW turbine [11], which is easily accessible and well documented, has been chosen as the test turbine.

Power output and blade loading are examined in order to reveal whether the oscillating waves will change the performance of the wind turbine. This could have consequences for both power harvest and fatigue considerations.

4. Methods and calculations

In [12] a method for wave simulations with the help of deforming mesh was established. This method is further developed by the inclusion of the horizontal wave particle movement as well as the vertical movement, and the discretization schemes for the numerical simulations are also slightly changed. Subsequently the Simulator for Offshore Wind farm Application (SOWFA) [13], developed at NREL, was modified in order to be integrated with the method for wave simulations. The result is a CFD set up that is suitable to study implications of wave movements on the wind flow and directly study the effect on a wind turbine or a wind farm. Hereafter, this set up will be referred to as the wave influenced wind turbine simulations (WIWiTS).The simulations are incompressible and transient with an unsteady Reynolds-averaged Navier-Stokes (URANS) approach. As turbulent closure, we have used the standard k-epsilon model [14].

4.1. Wave generation by the use of moving mesh

The method allows a description of a single sinusoidal wave on the ground patch in the simulation domain or a multiple of sinusoidal waves. Different waves can have different properties as well as different angles to each other and hence it is possible to describe a real wave spectrum on the surface. In this paper, only single sinusoidal waves are studied. This is of cause a simplification of a realistic sea. At the current stage of this study, we need to simplify the problem and focus on the swell conditions - primarily because this is the case when wind and waves can occur with different angels to each other, but also because this wave state is fairly well approximated with a pure sinusoidal form. Others have studied wave influenced wind by the use of coordinate transformation [15], but the method simulating wave influenced wind by the use of a moving mesh approach is believed to be unique in the context of offshore wind energy.

The open source CFD toolbox OpenFOAM [15] is used for both mesh generation and computations. By using a moving mesh approach, several sinusoidal waves can be implemented on the form;

$$\eta(x,t) = a\left\{\sin\left(2\pi(\frac{t}{T}-\frac{x}{L})\right) + \cos\left(2\pi(\frac{t}{T}-\frac{x}{L})\right)\right\} \quad (4)$$

where η is the sea surface elevation at a horizontal distance x at a given time t. a is the wave amplitude, T the wave period and L the wave length. Each grid cell moves up and down, reaching its maximum elevation in different time increments according to a sinusoidal function, and the movement looks like a wave propagating - much like the surface particles in a real ocean wave. A new solver was developed in the OpenFOAM tool box and named 'pimpleDyWFoam'. No deformation due to the wind force is allowed as the moving wave is seen as a solid wall. The wave properties and boundary conditions are listed in table 1 and 2. For more details regarding the moving wave method, reference is made to [12].

Before introducing the wind turbine in the simulations, the wind field over the waves was studied, using a less computationally demanding set up in two-dimensions. The purpose was to examine the required domain size, resolutions and the flow responses without wind turbine influences. The moving wave introduces some boundary effects close to the inlet and outlet part of the simulation grid. Even if the wave develops gradually after 10 sec of simulations and grows gradually to the prescribed amplitude size after 50 meters, these boundary effects are detectable. These effects come from the fact that the wave originates from one side of the domain and decays on the other side. In a large horizontal domain these boundary effects will not influence the core area of the domain.

Several domain sizes and wave states were tested and here we present results with a domain size of 1200 meters length and 400 meters height for four different cases. In order to ensure that the waves were properly resolved without too much computational resources a graded mesh was used where the cells near the surface are three times as small as the cells near the top. The smallest cells width close to the wave surface was approximately 1.5 meters. The mesh was generated with the openFOAM specific tool 'blockMesh'.

A logarithmic wind profile with the wind speed of 8 m/s at a reference height of 400 m is used as the inlet wind speed for all cases.

Table 1. The four different simulation cases without wind turbine representation

case	Decription	Wave parameters	Wave age
1a	wind and swell in the same direction	a = 4 m, L = 50 m, c = 8.8 m/s	1.5
1b	wind and swell in the opposite direction	a = 4 m, L = 50 m, c = -8.8 m/s	1.5
2a	wind and swell in the same direction	a = 4 m, L = 100 m, c = 12.5 m/s	2.1
2b	wind and swell in the opposite direction	a = 4 m, L = 100 m, c = -12.5 m/s	2.1

4.2. Actuator line method in SOWFA

SOWFA is a powerful tool for offshore wind power plant simulations, which includes both a model to run precursor atmospheric simulations and an actuator line turbine model, as well as an integration to the aeroelastic computer-aided engineering tool for horizontal axis wind turbines, FAST. This work uses only the actuator line part of SOWFA (which includes the 'pisoFoamTurbine' solver). Originally SOWFA was based on large scale eddy simulations (LES). The code is here changed to URANS in order to be compatible with the moving wave simulations.

The actuator line model in SOWFA relies on various input parameters. The Gaussian width parameter is an input parameter that controls how the forces are distributed along the lines representing the rotors. The number of the actuator line elements on a rotor blade need also to be chosen. Both these two parameters rely on the mesh and on the rotor characteristics. In [17] various testing of best suitable input parameters was performed. In this way the model was "tuned" to given results. This is not possible in the present study and the value of the input parameters is chosen based on best practice. The NREL 5 MW turbine is assumed to produce power close to 2 MW with a reference wind

speed of 8 m/s and a rotation speed of approximately 9 RPM [18]. The turbine rotational speed is set to 9 RPM. The wind speed at the hub height will be influenced by the wave and the resulting wind speed at hub height will be lower than 8 m/s and the simulated power should be less than 2MW. A variable-speed controller is incorporated in the SOWFA actuator line model. In these simulations the turbine will operate in underrated wind and try to optimize the power capture. In this region the generator torque should be proportional to the square of the filtered generator speed [11].

The turbine properties and input parameters are listed in table 1. For more details regarding the actuator line method in SOWFA, reference is made to [13, 17, 18 and 19].

4.3. Combined simulations; wave influenced wind turbine simulations - WIWiTS

The wave simulations described in 4.1 were coupled with the turbine simulations described in 4.2. Hence, a new combined CFD simulation was developed. This new solver embedded in the WIWiTS was named 'pimpleDyWTurbineFoam'.

Grid dependency studies performed on the two dimensional set up (without turbine representation) showed that in order to have grid independent solutions a very fine mesh is preferable. Also the domain needs to be large to minimize boundary effects. This resulted in hundreds of millions of cells when used on an equivalent three dimensional case. Simulations on such a mesh were not feasible. The mesh was instead constructed with a background graded mesh of same resolutions as in the wave simulations without wind turbine (described in section 4.1) and a refined area around the turbine rotor as a necessary compromise between the domain size and the resolution of the grid (see figure 1). The simulation domain was 600 m long, 260 m wide and 400 m high. This is believed to be too short to avoid all boundary effects, but the simulations will nevertheless give indications on the relative differences in power generation for different wave conditions compared to a no-wave situation.

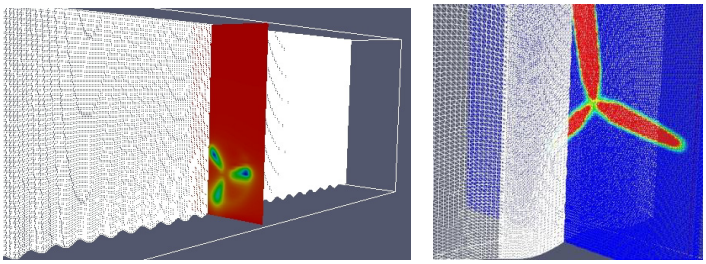

Fig.1. Illustration of the WIWiTS domain, turbine size is exaggerated (left). The WIWTS mesh is graded near the surface and refined in a region around the turbine (right).

The turbine will rotate in a mesh with changing grid cell size. The input parameters should be a ratio of the grid cell size. Troldborg [20] recommends that the Gaussian width parameter should be larger than twice the local grid cell length. In all three cases the Gaussian width parameter is 2.85 times larger than the smallest local grid cell length and 0,98 times larger than the largest grid cell length. The largest grid cell length is located in the very top of the domain and the rotor will not experience the largest grid cells. [19] recommended that for each grid cell across the blade, there should be at least 1.5 actuator line elements. In these cases the airfoil is divided into 40 elements. The implication is that for every local grid cell there are between 0.78 and 2.24 actuator line elements depending on what part of the grid the rotor experiences. Thus the vertically graded grid resolution gives problems in estimating the right input values for the turbine simulations. It will nevertheless be interesting to compare the results since this will be discussed in light of a control run over a flat surface that is performed on the same grid as the simulations with the wave movements. The results of the WIWTS simulations should serve as a demonstration of the relative influence the wave modified wind profiles could have on the wind turbine performance.

Only the wave with wave age 2.5 is used together with the wind turbine. The reason for this choice is that this is a

more realistic swell condition although the wave amplitude will be higher than what can normally be expected. Wind turbine performance for three different cases are presented as listed in table 2: wind and swell in the same direction, wind and swell in the opposite direction and wind over surface with low roughness (no waves).

The WIWiTS input parameters and boundary conditions are presented in table 2 and 3. In section 5, we emphasize on the wind velocity and the turbulent kinetic energy because this is the most important flow parameters when studying turbine performance. Tests have been made to find the minimum simulation time required for the flow to reach a quasi-stationary stage and, based on the tests, a simulation time of 300 seconds should be enough.

Table 2. The three different simulation cases with wind turbine representation

case	Description	Wave parameters	Wind at inlet
a	wind and swell in the same direction	a=4 m, L=100m, c=12,5 m/s	8 m/s
b	wind and swell in the opposite direction	a=4 m, L=100m, c= -12,5 m/s	8 m/s
c	wind over a surface with low roughness	No wave, z_0 = 0,0002 m	8 m/s

Table 3. Boundary conditions on the different patches for the WIWTS, with OpenFoam specific naming. On the ground patch the boundary conditions for U will be different in the case of a flat surface (fixedValue) compared to a moving wave surface (movingWallVelocity).

field		Inlet	outlet	top	sides	Ground
U	wind velocity	ABLvelocity*	zeroGradient	slip	slip	movingWallVelocity fixedValue
p	pressure	zeroGradient	fixedValue	slip	slip	zeroGradient
k	turbulent kinetic energy	fixedValue	zeroGradient	slip	slip	kqRWallFunction
epsilon	turbulent dissipation of energy	fixedValue	zeroGradient	slip	slip	epsilonWallFunction;
nut	viscosity	fixedValue	zeroGradient	slip	slip	nutkRoughWallFunction

*Full openFOAM specific name: atmBoundaryLayerInletVelocity

5. Results and discussion

First, an examination of two different wave states with the same inlet wind is presented in section 5.1. Thereafter the turbine is introduced in the domain and power generation and some examples of blade loading are presented in 5.2.

5.1. Wind velocity and turbulence profiles without turbine representation

Both the wind profile and the turbulent kinetic energy profiles will depend on the direction of the wave relative to the incoming wind field. In Figure 2 and 3 results from simulations with wave ages, 1.5 and 2.1 (listed in table 1) are shown. The figures show the sampling of instant horizontal and vertical wind velocity profiles for every second between 251-300 seconds of simulations. During this runtime, the simulations have reached a quasi-steady state. Figure 4 shows the corresponding turbulent kinetic energy profiles. The sampled data are from the middle of the domain (x=600 m) where boundary affects are negligible.

The wave movement periodically modifies the wind profiles up to approximately 100 metres over the sea surface. The waves with wave age 1.5 are the shortest and steepest wave generating more turbulence, and variations in the lowest meters compared to the wave with wave age 2.1. The latter moves faster with longer wave lengths and this wave state induce variations at the highest levels. The vertical velocity fluctuations are identifiable up to 100 metres.

For both cases the wind profile in the opposed situation shows an ‘overshoot’ of the wind speed compared to the logarithmic inlet and also compared to the aligned situation. This is believed to be due to the fact that the extra generated turbulence in the opposed case gives rise to a ‘richer’ profile near the surface and further up in the MABL. In other words The short and steep wave (case 1a and 1b in table 1) gives higher turbulence values and the overshoot is more pronounced than in the longer wave case (case 2a and 2b, table 1).

It should be noted that the turbulence profiles indicate little or no vertical mixing from approximately 75 m and upwards, whereas the velocity profiles show slight variations above this level. The true turbulence level is a combination of the large-scale motion generated by the waves as well as the turbulence predicted by the k-epsilon model. In Figure 4 only the filtered k values directly obtained from the k-epsilon model is shown. One should also account for the large-scale variances and calculate the turbulent kinetic energy contribution from this. In order to do so, time averaging must be enabled in the CFD simulations and this has not been done. The turbulence result presented in Figure 4 should thus be interpreted with care.

Since the gradient of both the horizontal and vertical velocity profiles is close to zero at the top of the domain, it is a valid assumption that the domain height is high enough and that the overshoot represent a physical sound flow response in the cases where a wave opposes the wind field.

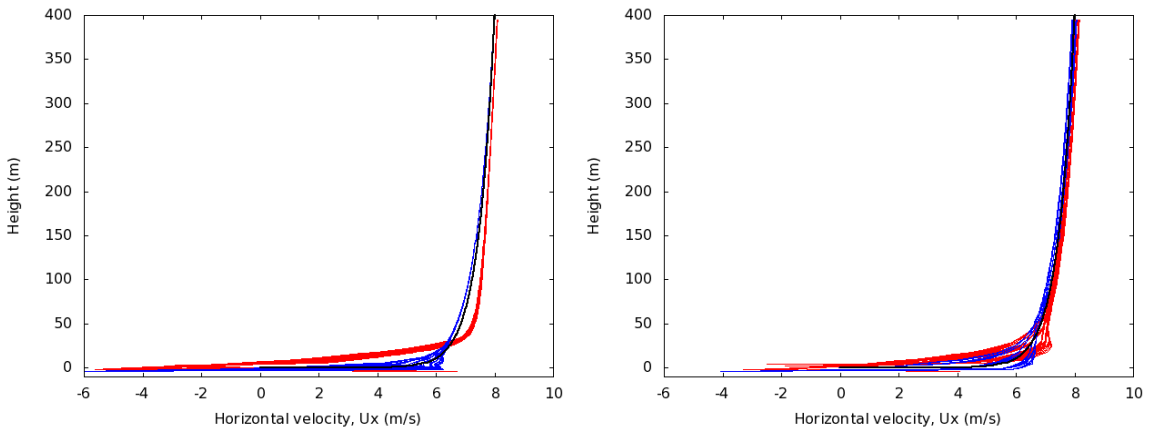

Fig. 2. Profile of horizontal wind (m/s). Wind and wave in the same direction (blue), wind and wave in the opposite direction (red) and the logarithmic inlet wind velocity (black). Profiles are sampled from the middle of the domain (x=600 m) for every second between 251-300 seconds of simulations. Case 1a and 1b, see table 1 (left) and case 2a and 2b, see table 1 (right).

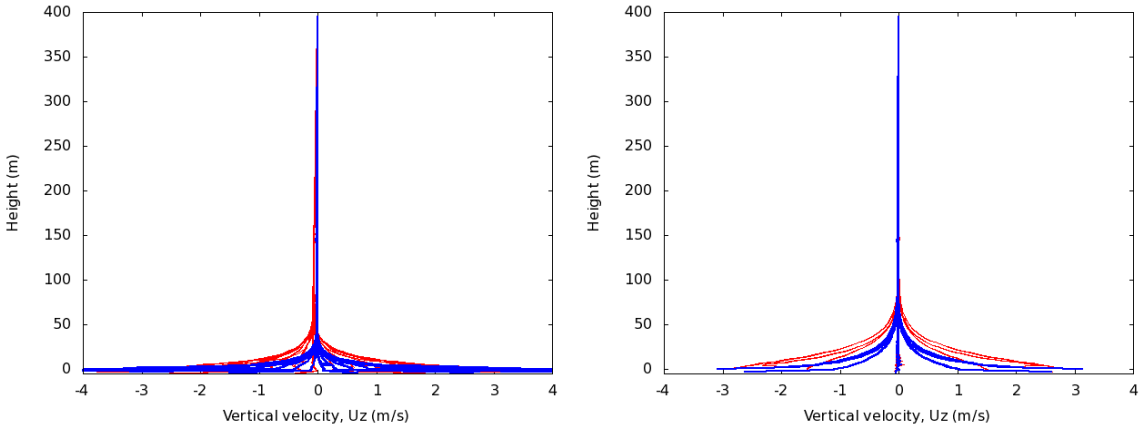

Fig. 3. Profile of vertical wind (m/s). Wind and wave in the same direction (blue), wind and wave in the opposite direction (red). Profiles are sampled from the middle of the domain (x=600 m) for every second between 251-300 seconds of simulations. Case 1a and 1b, see table 1 (left) and case 2a and 2b, see table 1 (right).

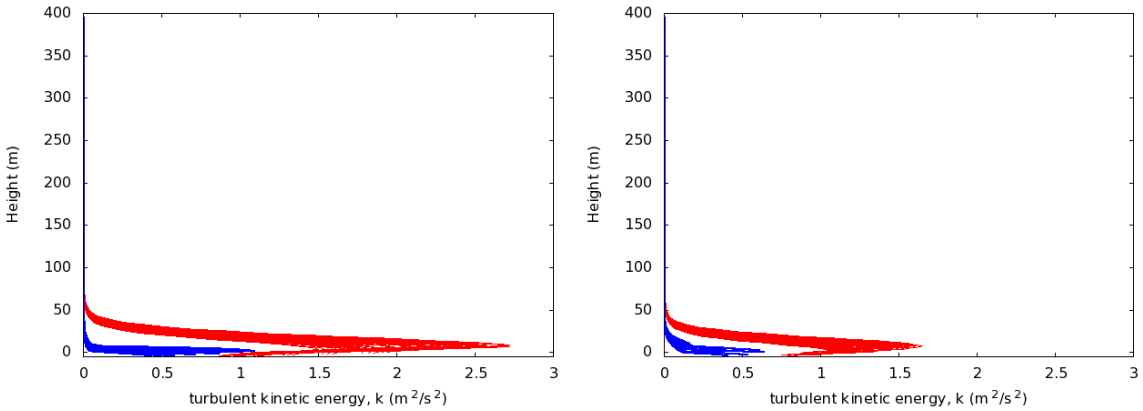

Fig. 4. Profile of turbulent kinetic energy, k (m^2/s^2), directly obtained from the k-epsilon model. Wind and wave in the same direction (blue), wind and wave in the opposite direction (red). Profiles are sampled from the middle of the domain (x=600 m) for every second between 251-300 seconds of simulations. Case 1a and 1b, see table 1 (left) and case 2a and 2b, see table 1 (right).

5.2. Power generation and blade loading

For every simulations time step "global" turbine quantities i.e. rotor power (W), thrust (N), and "local" blade quantities, i.e. axial force (N), tangential force (N), will be calculated and stored. In Figure 5 produced power are shown for the three cases a, b and c. The power will oscillate for cases a and b where the swell is present, but for case c where the wind flow is over a flat surface, the same oscillations are not present. There will always be some minor variations in the power curve and this is believed to be code specific and dependent on how the user defines the parameters mentioned in section 4.3 [18]. The oscillations in cases a and b have the same frequency as the wave. The simulation for case c, over the flat surface, is performed on the same grid as for cases a and b. Therefore it seems that these oscillations are a consequence of the wave movements.

In Figure 5 the generated power is higher in case b that in case a and c. This is linked to the fact that the fast moving swell generates a "richer" profile in case b, as mentioned in 5.1. When introducing the turbine in the domain the domain height of 400 m seems to short. The turbine represents an 'obstacle' and generates more turbulence and a more complicated flow behavior than case the case with only waves. The power curve seems to reach a stable

development for case a and c after approximately 170 sec, but for the b case a slight increase in generated power can be detected after approximately 250 sec. This can be an indication that the simulation time are too short for the opposed case. Because of the limitation in number of grid cells, we could not 'afford' to put the turbine in the middle of the domain in a 1200 wide domain where no boundary effects were present. Instead, the turbine needed to be placed far downstream in the domain. By doing so, we cannot exclude boundary effects entirely and this has to be taken into considerations when interpreting the results.

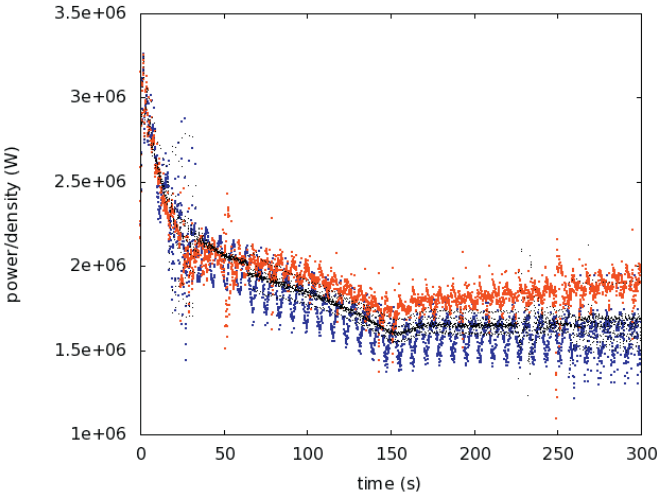

Fig. 5. Generated rotor power per density (Wm^3/kg) for the three different cases; wind and swell in the same direction (blue), wind and swell in the opposite direction (red) and wind over a surface with low roughness (black). The simulation time was 300 sec. Noise in the curves are due to start up effect every time the simulations had to be restarted due to technical problems.

In Figure 6-8 the forces in the rotor rotational tangential direction (hereafter named the tangential force) on each blade are shown for two different time steps. The left graph in every figure corresponds to 334 seconds and the right graphs are plotted half a wave period later, i.e. at 338 seconds. This will give a picture of the variation in the tangential force on each blade during two different wave positions. There are slightly more spread in the forces in case a – when the wave is aligned with the wind. Case b – with waves is opposing the wind, gives larger forces than case a and c.

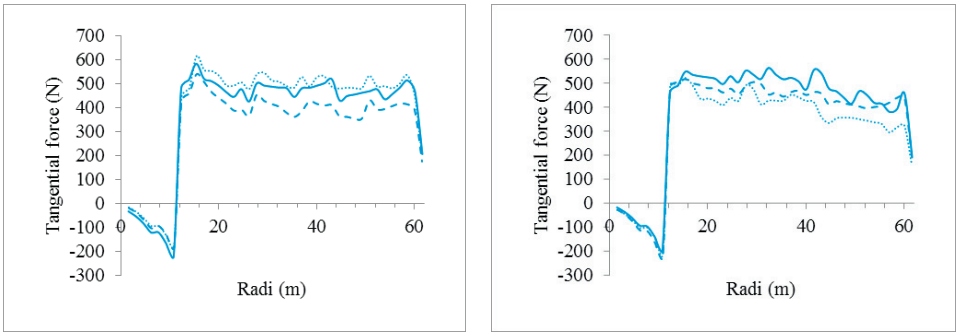

Fig. 6. Case a) Aligned situation. Tangential force (N) along the rotor blade for each blade 334 sec (left) and 338 sec (right). Blade 1 – solid line, blade 2 - broken line, blade 3 - dotted line.

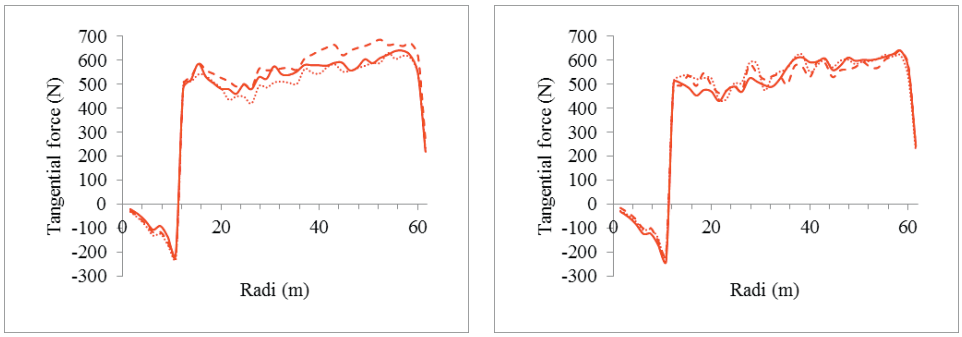

Fig. 7. Case b) Oppose situation. Forces in the rotor rotational tangential direction (N) along the rotor blade for each blade after 334 sec (left) and 338 sec (right). Blade 1 – solid line, blade 2 - broken line, blade 3 - dotted line.

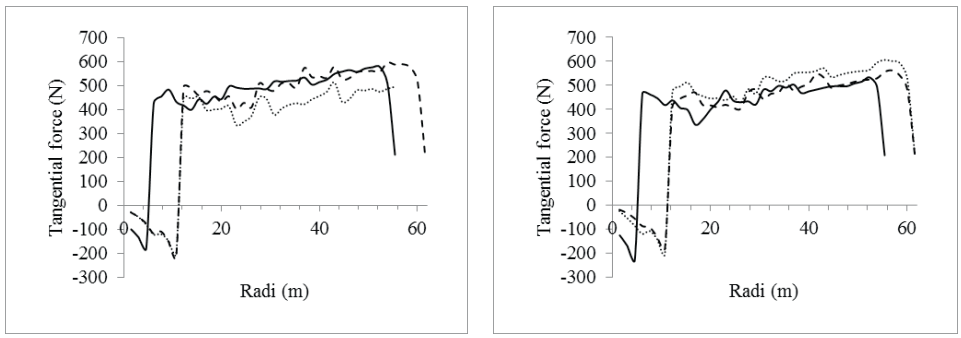

Fig. 8. Case c, flat surface. Forces in the rotor rotational tangential direction (N) along the rotor blade for each blade after 351 sec (left) and 355 sec (right). Blade 1 – solid line, blade 2 - broken line, blade 3 - dotted line.

6. Conclusions and suggestion for future studies

A combined CFD set up where an actuator line representation of a turbine operates in wave influenced wind is developed. These WIWiTS results show that wave influenced wind affects the wind turbine performance.

Before introducing the wind turbine in the simulation domain, wave simulations on a two-dimensional set up were conducted. These simulations showed that the influence of the wave extend tens of meters up in the atmosphere and will affect the wind in the swept area of wind turbines. Several simulations were performed and some general observations is that in a fast moving swell regime a wave that oppose the wind field will create larger turbulence levels (predicted directly from the k-epsilon model) than if the wave was aligned with the wind or with no wave present. More detailed turbulence analyses are however required to investigate this phenomenon further. When working with URANS predictions from the k-epsilon model, the results should be coupled with turbulence calculations related to the large-scale motion generated by the waves. This should be topic for future work and improvements.

The wave movements result in oscillations in the power output when the turbine operates in underrated wind with a torque controller. The wave movements periodically modify the wind profiles up to approximately 100 metre over the sea surface. The wind turbine with the nacelle at 88 metre height with rotor radius of 61 metre will experience these fluctuations and it will lead to slightly larger tangential forces than comparable situations over a flat surface. Also more spread in the forces was observed when the wind and the wave was aligned to each other.

There are indications that the domain is too small for the WIWiTS and complete grid independence was not reached. Therefore these results can only serve as an indication of the impact wave influenced wind may have on wind turbine performance. Nevertheless, it is interesting to note the relative differences between conditions with swell aligned with

the wind field, opposing the wind field and over a surface with low roughness (no waves). The swell shown has amplitude of 4 metre and it is unrealistic that such a large swell will persist for a longer time. More simulations with lower swell height and more realistic sea states are recommended.

The wave influenced wind will affect the turbine performance, as well as the loads, but it is not possible to conclude if this influence is significant in relation to the natural turbulent structure of the atmosphere and the varying atmospheric stability. We have here developed and demonstrated the use of a flexible open source CFD set up, and hopefully this will motivate further studies in this area.

Acknowledgements

This work was made possible by funding from the Norwegian Research Council Industrial PhD-program (198257) and from StormGeo. The work is also a part of the Norwegian Centre for Offshore Wind Energy (NORCOWE) under grant 193821/S60 from the Research Council of Norway (RCN). NORCOWE is a consortium with partners from industry and science, hosted by Christian Michelsen Research. The authors would like to acknowledge Theodor Ivesdal at the University of Stavanger for is outstanding technical help with the Linux cluster.

References

[1] Kalvig S, Gudmestad OT, Winther N. Exploring the gap between 'best knowledge' and 'best practice' in boundary layer meteorology for offshore wind energy. Wind Energy 2013;17(1). doi: 10.1002/we.1572

[2] Semedo A, Saetra Ø, Rutgersson A, Kahma KK, Pettersson H. Wave-induced wind in the marine boundary layer. Journal of the Atmospheric Sciences 2009;66:2256-2271.

[3] Ocampo-Torres F, García-Nava H, Durazo R, Osuna P, Díaz Méndez G, Graber H. The INTOA Experiment: A study of ocean-atmospher interactions under moderate to strong offshore winds and opposing swell conditions in the Gulf of Tehuantepec, Mexico. Boundary-Layer Meteorology 2011;138(3):433-451. doi: 10.1007/s10546-010-9561-5

[4] Lange B, Larsen S, Højstrup J, Barthelmie R. Importance of thermal effects and sea surface roughness for offshore wind resource assessment. Journal of Wind Engineering and Industrial Aerodynamics, Volume 92, Issue 11, September 2004, Pages 959-988, ISSN 0167-6105, http://dx.doi.org/10.1016/j.jweia.2004.05.005.

[5] Stull RB. An introduction to boundary layer meteorology. Vancouver: Atmospheric and Oceanographic Sciences Library, Springer; 1988.

[6]Barthelmie R J, Palutikof JP, Davies TD. Estimation of sector roughness lengths and the effect on prediction of the vertical wind speed profile. Boundary-Layer Meteorology 1993; 66(1-2):19-47. doi: 10.1007/BF00705458

[7] Motta M, Barthelmie RJ, Volund P. The influence of non-logarithmic wind speed profiles on potential power output at Danish offshore sites. Wind Energy 2005;8(2):219-236. doi: 10.1002/we.146

[8] Sathe A, Mann J, Barlas T, Bierbooms WAAM, van Bussel GJW. Influence of atmospheric stability on wind turbine loads. Wind Energy 2012;16(7). doi: 10.1002/we.1528

[9] Edson J, Crawford T, Crescenti J, Farrar T, Frew N, Gerbi G, Helmis C, Hristov T, Khelif D, Jessup A, Jonsson H, Li M, Mahrt L, McGillis W, Plueddemann A, Shen L, Skyllingstad E, Stanton T, Sullivan P, Sun J, Trowbridge J, Vickers D, Wang S, Wang Q, Weller R, Wilkin J, Williams AJ, Yue DKP, Zappa C. The coupled boundary layers and air-sea transfer experiment in low winds. Bulletin of the American Meteorological Society 2007;88(3):341-356.

[10] Sørensen JN, Shen WZ. Numerical modeling of wind turbine wakes. J. Fluid Eng. 2002;124:393-399. doi: 10.1115/1.1471361

[11] Jonkman J, Butterfield S, Musial W, Scott G. Definition of a 5-MW Reference Wind Turbine for Offshore System Development. National Renewable Energy Laboratory, Rept. NREL/TP-500-38060, Golden, CO, 2009.

[12] Kalvig S, Manger E, Kverneland R. A method for wave driven wind simulations with CFD. Energy Procedia 2013;35:148-156, ISSN 1876-6102, http://dx.doi.org/10.1016/j.egypro.2013.07.168

[13] Churchfield MJ, Lee S and Moriarty P. Overview of the simulator for offshore wind farm application (SOWFA) National Renewable Energy Laboratory, Golden, CO, USA 03 May 2012 http://wind.nrel.gov/designcodes/simulators/sowfa/ accessed January 2014.

[14] Launder BE, Spalding DB. The numerical computation of turbulent flows, Computer Methods in Applied Mechanics and Engineering, 3 (2), Pages 269–289, 1974, DOI: 10.1016/0045-7825(74)90029-2

[15] Sullivan PP, Edson JB, Hristov T, McWilliams JC. Large-eddy simulations and observations of atmospheric marine boundary layers above nonequilibrium surface waves. Journal of the Atmospheric Sciences 2008;65(4):1225-1245.

[16] OpenFOAM; http://www.openfoam.com/ (retrieved 09.01.2014)

[17] Kalvig S, Manger E, Hjartager B. Comparing different CFD wind turbine modelling approaches with wind tunnel measurements. IOP conference Series. In review.

[18] Churchfield MJ, Lee S, Michalakes J, Moriarty PJ. A numerical study of the effects of atmospheric and wake turbulence on wind turbine dynamics. Journal of Turbulence 2012. doi: 10.1080/14685248.2012.668191

[19] Martínez LA, Leonardi S, Churchfield MJ, Moriarty PJ. A comparison of actuator disc and actuator line wind turbine models and best practices for their use. 50th AIAA Aerospace Sciences Meeting and Exhibit, Nashville, TN, Jan. 9–12, AIAA, Washington D.C., 2012.
[20] Troldborg N. Actuator line modeling of wind turbine wakes. PhD Thesis 2008, Technical University of Denmark, Lyngby, Denmark.